Supplementary information for

Oxygen enriched porous carbon nanoflakes enable high-performance zinc ion hybrid capacitors

Taiyu Cao, Chunliu Zhu*, Xinyu Wang, Zhaowei Ji, Huanyu Liang, Jing Shi, Weiqian Tian, Jingwei Chen, Jingyi Wu, Huanlei Wang*

School of Materials Science and Engineering, Ocean University of China, Qingdao 266100, China.

*Corresponding author.

E-mail: huanleiwang@ouc.edu.cn, 1339724402@qq.com;

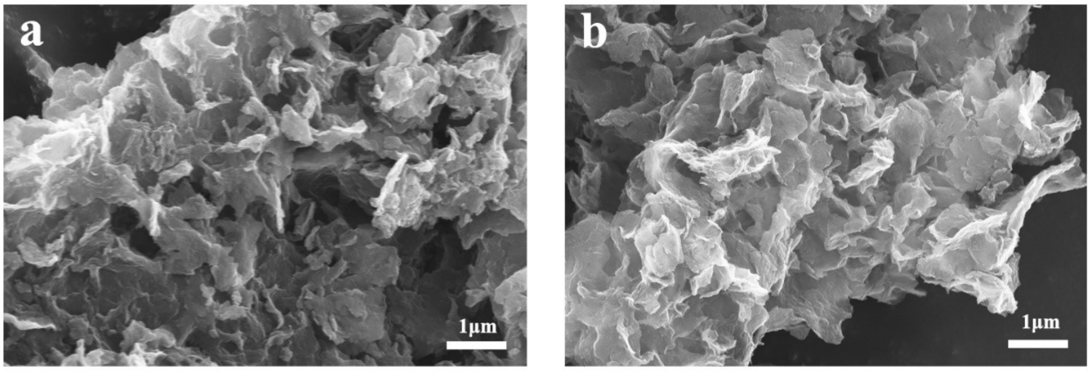

Fig. S1 SEM images of (a) PCNs-700 and (b) PCNs-900.

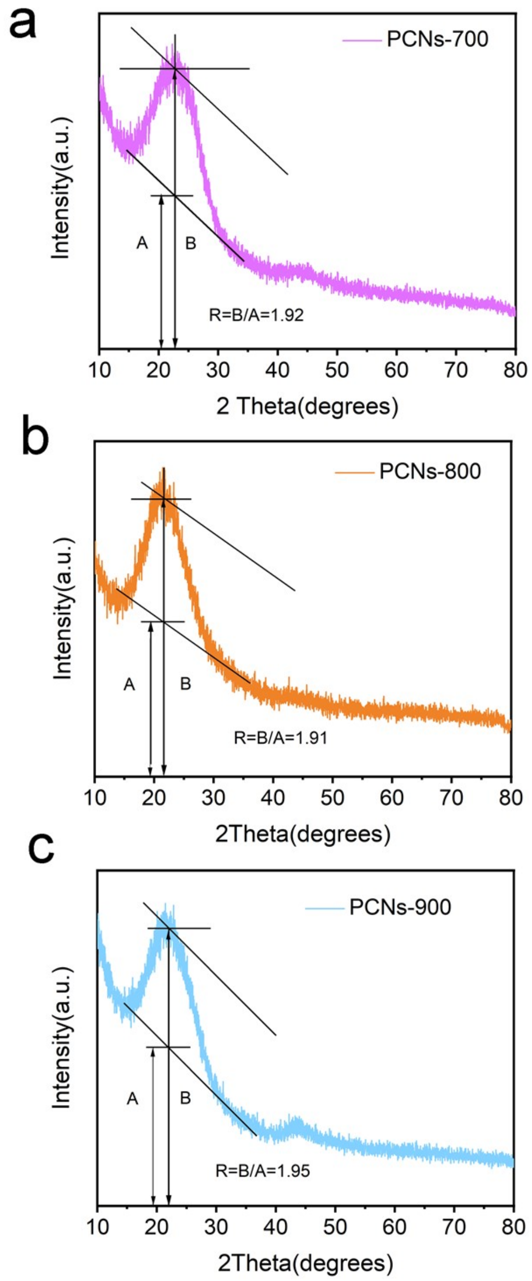

Fig. S2 XRD patterns of (a) PCNs-700, (b) PCNs-800, and (c) PCNs-900.

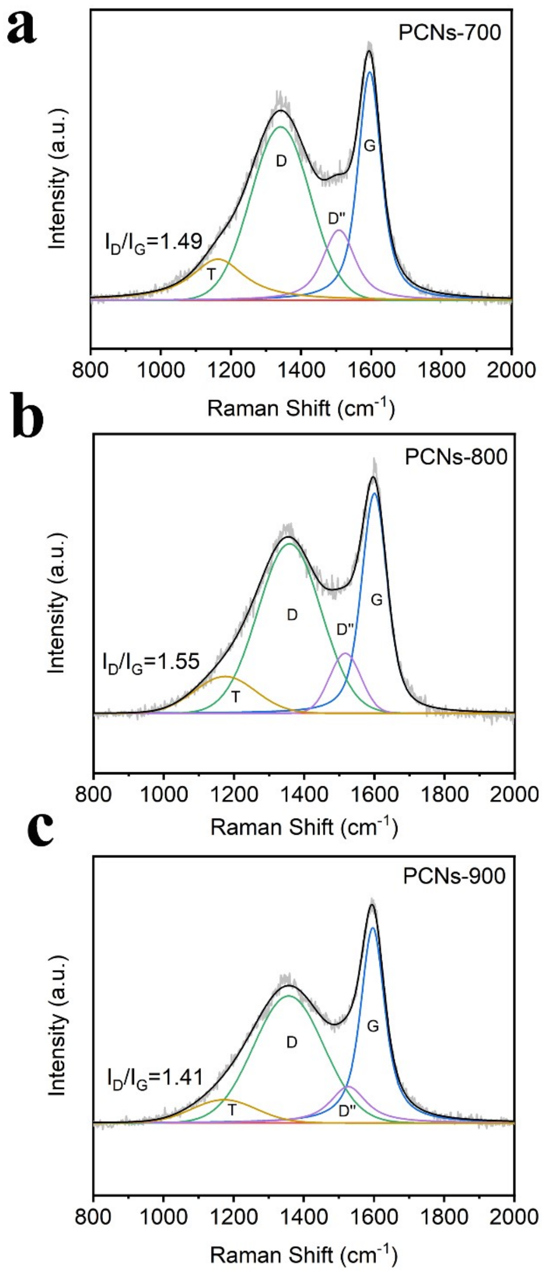

Fig. S3 Raman spectra of (a) PCNs-700, (b) PCNs-800, and (c) PCNs-900.

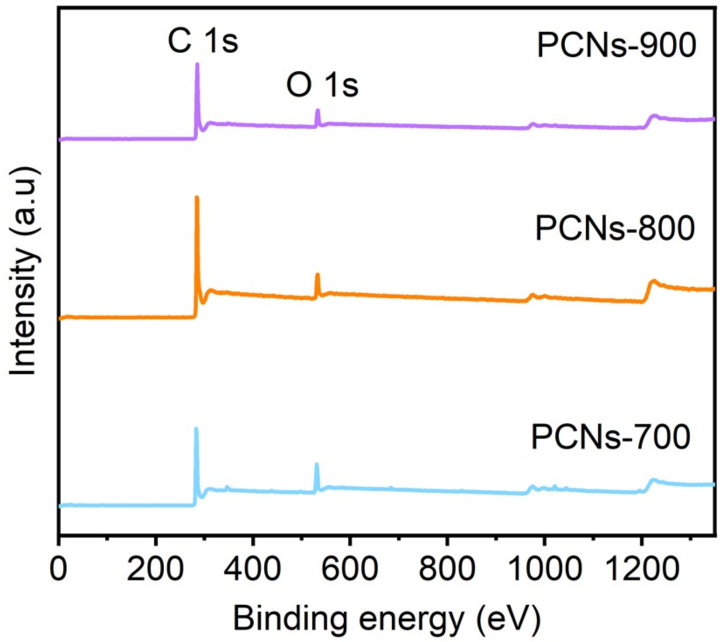

Fig. S4 XPS survey spectra of PCNs-700, PCNs-800, and PCNs-900.

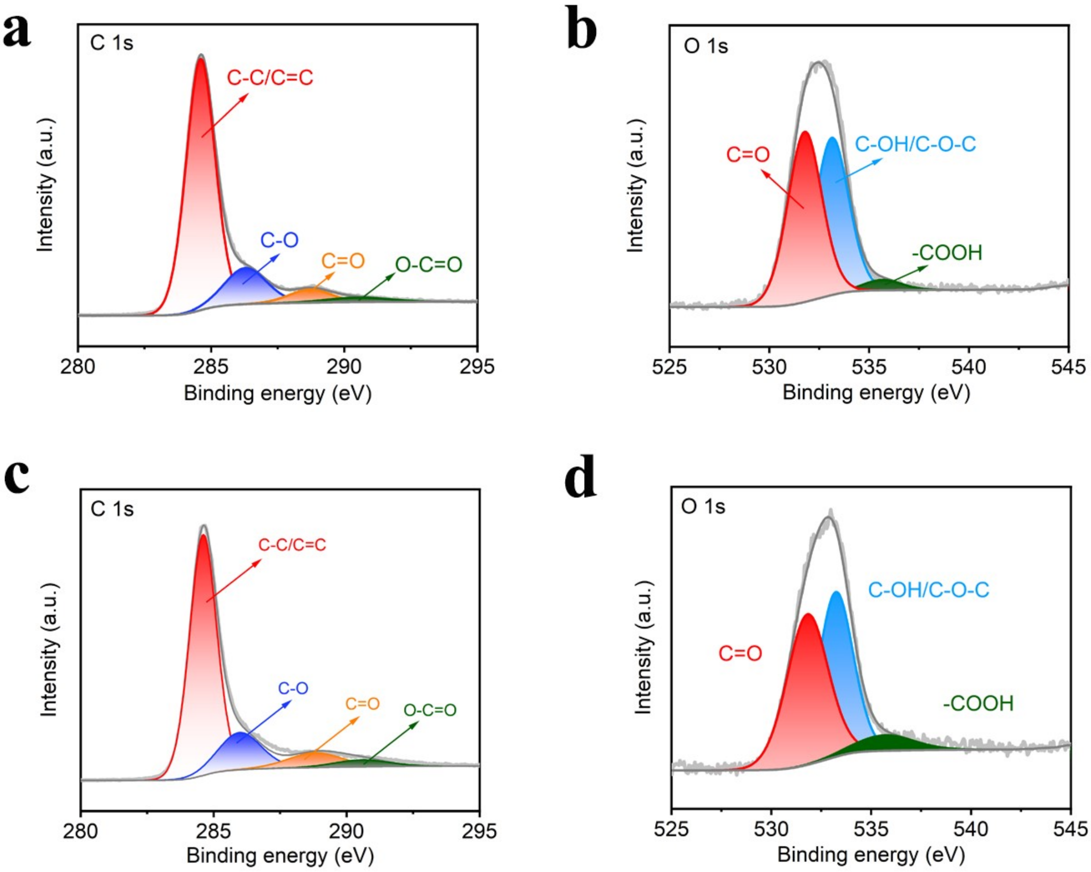

Fig. S5 High resolution (a) C 1s and (b) O 1s spectra of PCNs-700; High resolution (c) C 1s spectra and (d) O 1s spectra of PCNs-900.

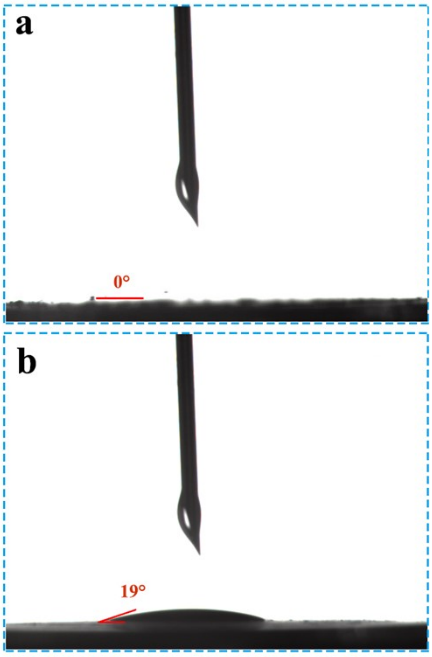

Fig. S6 Water contact angles of (a) PCNs-800, and (b) commercial activated carbon (YP-50F).

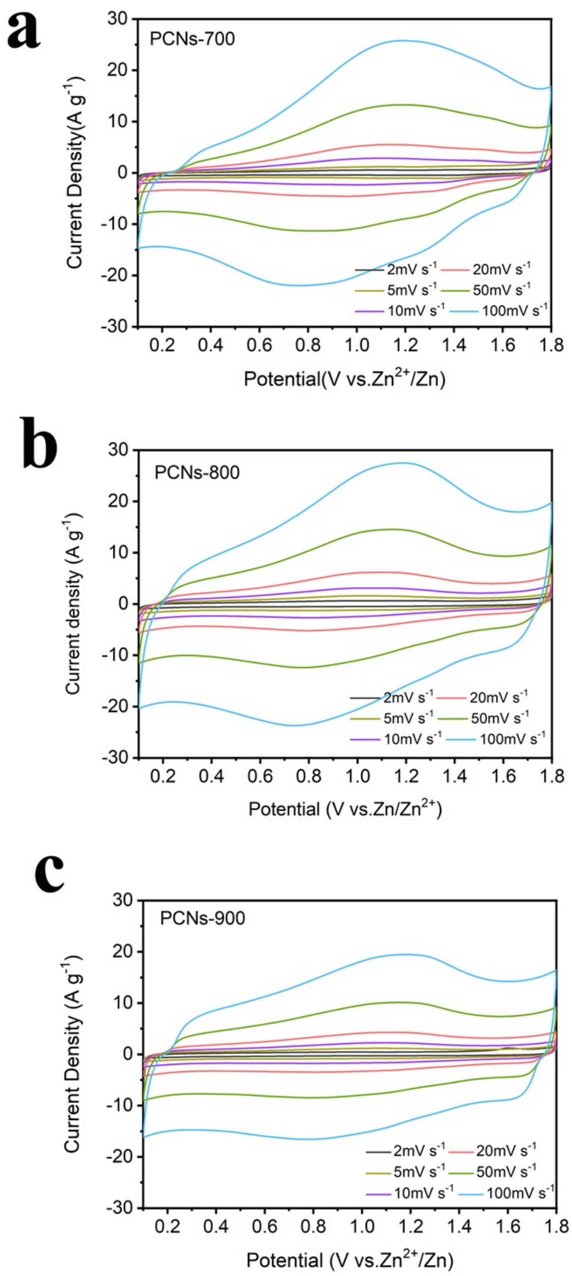

Fig. S7 CV curves of (a) PCNs-700, (b) PCNs-800, and (c) PCNs-900 based ZIHCs at scan rates range of 2-100 mV·s^{-1}.

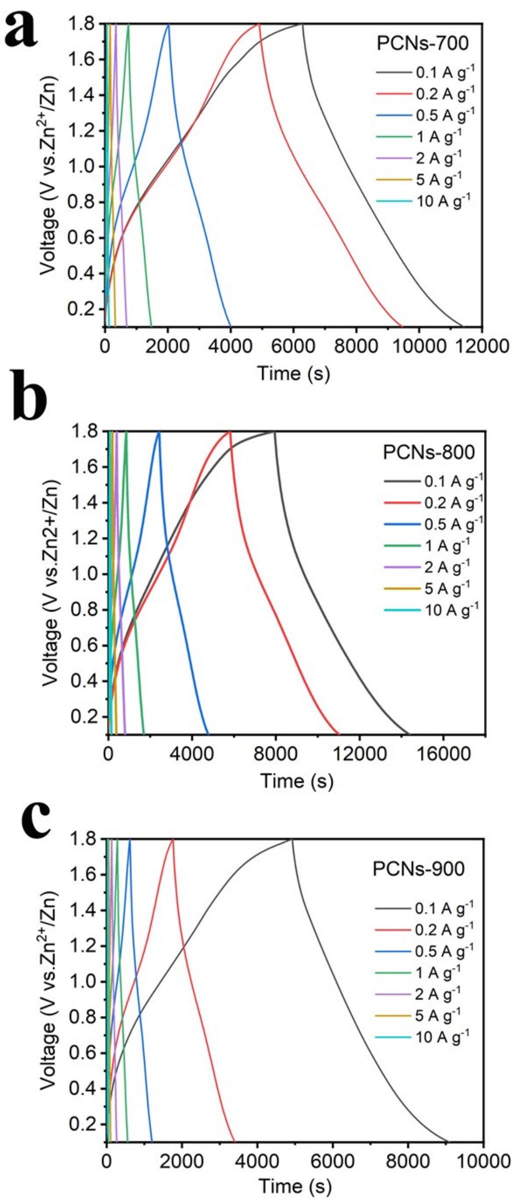

Fig. S8 Galvanostatic charge–discharge profiles at 0.1-10 A g^{-1} for (a) PCNs-700, (b) PCNs-800, and (c) PCNs-900.

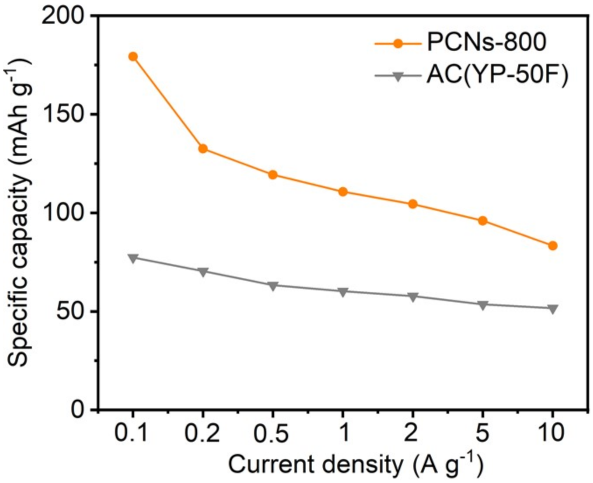

Fig. S9 Comparison for rate capability between PCNs-800 cathode and commercial activated carbon (YP-50F).

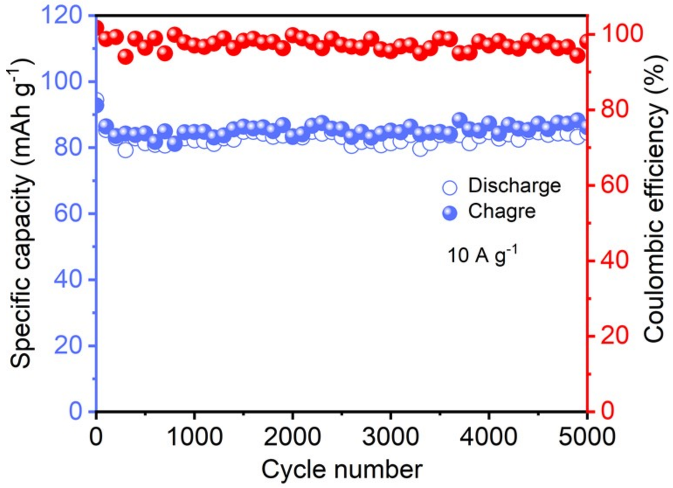

Fig. S10 Cyclic performance of PCNs-800 at 10 A g^{-1}.

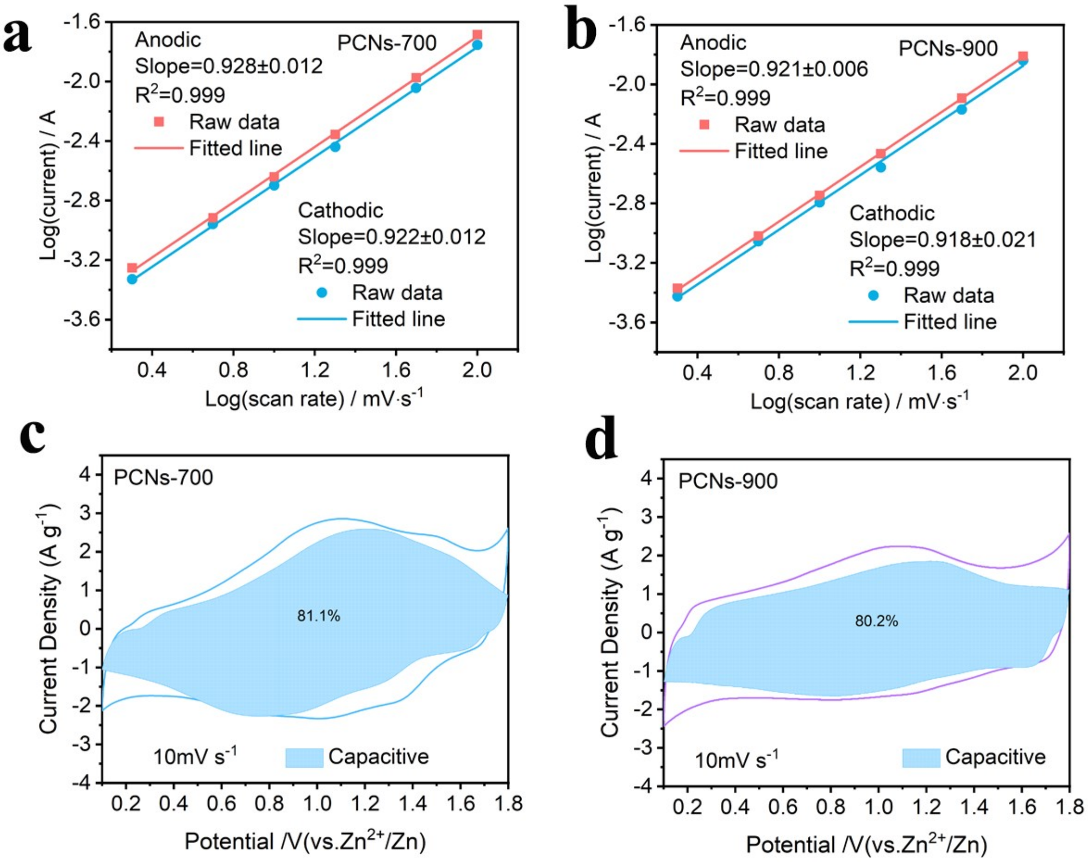

Fig. S11 Selected cathodic and anodic *b* values of peak currents for (a) PCNs-700, and (b) PCNs-900; Capacitive contribution of (c) PCNs-700 and (d) PCNs-900 cathodes-based ZIHCs at 10 mV s^{-1}.

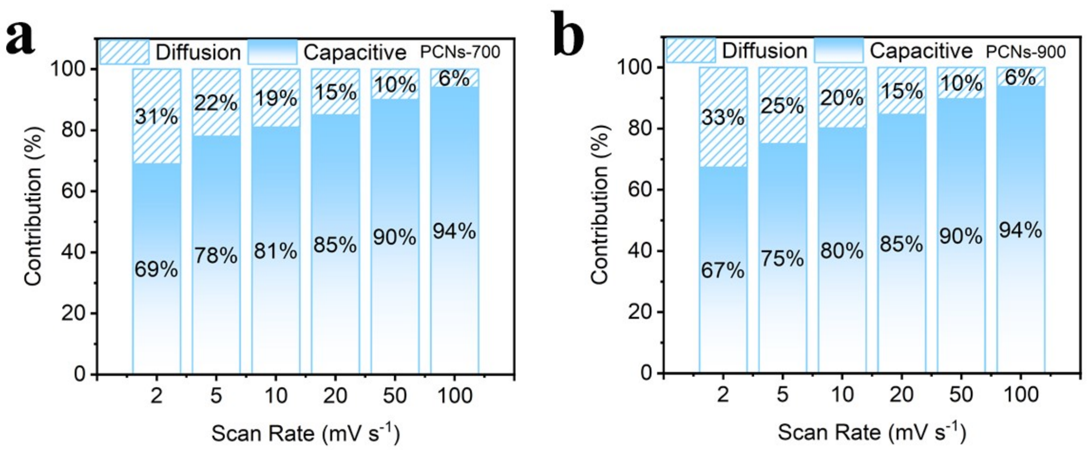

Fig. S12 Capacitive/diffusion contribution ratios of (a) PCNs-700 and (b) PCNs-900 at different scan rates.

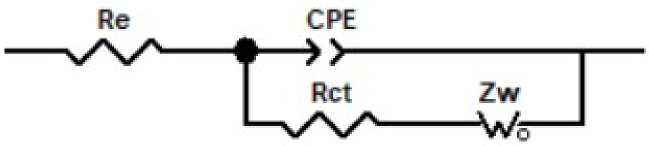

Fig. S13 The corresponding simulating equivalent circuit.

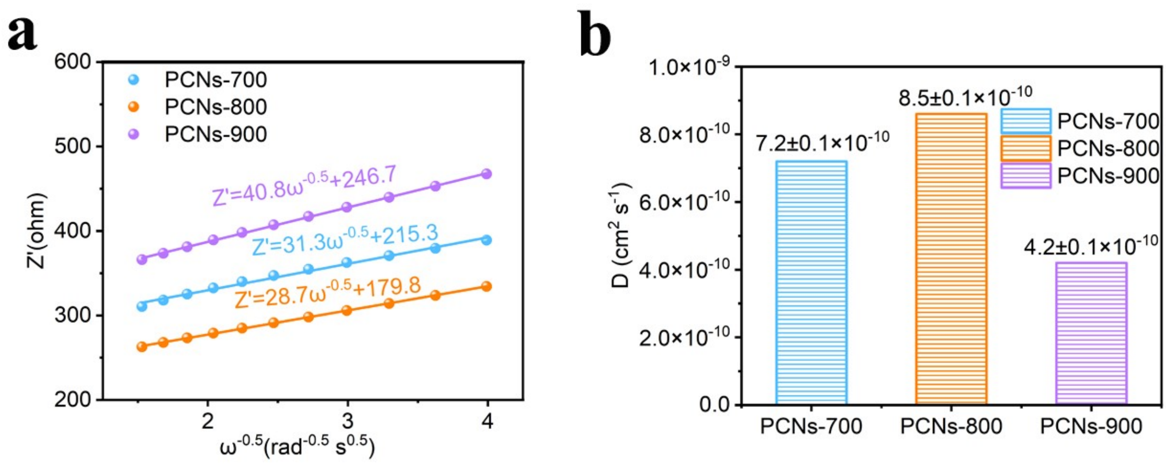

Fig. S14 (a) Linear plots of real resistances (Z') against angular frequencies ($\omega^{-0.5}$) in the low-frequency region for PCNs-700, PCNs-800, and PCNs-900, respectively. (b) Ion diffusion coefficients of PCNs-700, PCNs-800, and PCNs-900.

The diffusion coefficient of ions could be calculated by the EIS technique based on the following formulas[1-3]:

$$Z^{'} = \sigma\omega^{-0.5} + R_e + R_{ct} \quad \text{(S1)}$$

$$D_{Zn^{2+}} = \frac{R^2T^2}{2A^2F^4C^2n^4\sigma^2} \quad \text{(S2)}$$

where Z' is real part of impedance (Ω), ω is angle frequency (rad s^{-1}), σ is diffusion resistance (Ω $s^{-0.5}$), R_e is ohmic resistance between the electrode and electrolyte (Ω), R_{ct} is charge transfer resistance (Ω), n is electron transfer numbers per molecule during electron reaction, D is ion diffusion coefficient (cm^2 s^{-1}), A is the surface area of electrode (cm^2), R is gas constant (8.314 J mol^{-1} K^{-1}), T is Kelvin temperature (293.15 K), C is molar concentration of electrolyte (mol L^{-1}), and F is Faraday constant (96485 C mol^{-1}).

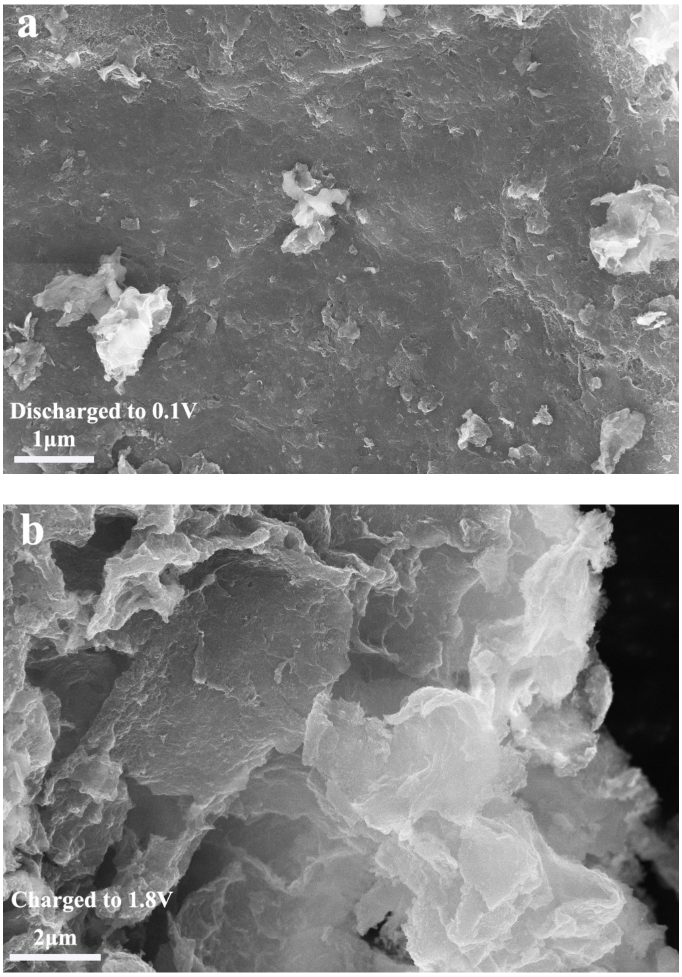

Fig. S15 *Ex-situ* SEM of PCNs-800 electrode at (a) discharged and (b) charged states.

Table S1 Physical and chemical parameters for PCNs-700, PCNs-800, and PCNs-900.

Samples	***R***	I_D/I_G	S_{BET}[a] (m^2 g^{-1})	V_t[b] (cm^3 g^{-1})	**Pore volume (%)**		**XPS composition (at%)**	
					V<2nm	**V>2nm**	**C**	**O**
PCNs-700	1.92	1.5	757	1.13	14	86	86.5	13.5
PCNs-800	1.91	1.6	1134	1.41	15	85	81.0	19.0
PCNs-900	1.95	1.4	532	1.03	6	94	91.2	8.8

[a)] Surface area was calculated by BET method;

[b)] The total pore volume was determined by DFT method

.

Table S2 Specific capacities of PCNs-800 and other reported cathode materials for ZIHCs.

Cathode (Specific surface area)	Low rate specific capacity	High rate specific capacity	Mass loading	Ref.
PCNs-800 (1134 m^2 g^{-1})	179 mAh g^{-1} at 0.1 A g^{-1}	83 mAh g^{-1} at 10 A g^{-1}	~1.0 mg cm^{-2}	This Work
SOCN-10 (1877 m^2 g^{-1})	151 mAh g^{-1} at 0.1 A g^{-1}	80 mAh g^{-1} at 10 A g^{-1}	-	3
PHC3 (1469.3 m^2 g^{-1})	149 mAh g^{-1} at 0.1 A g^{-1}	88 mAh g^{-1} at 10 A g^{-1}	~2.3 mg cm^{-2}	4
S-O-PC-HB (818.17 m^2 g^{-1})	107.5 mAh g^{-1} at 0.2 A g^{-1}	14 mAh g^{-1} at 10 A g^{-1}	~1.0 mg cm^{-2}	5
Zn-MET-800 (651.6 m^2 g^{-1})	164 mAh g^{-1} at 0.1 A g^{-1}	64 mAh g^{-1} at 10 A g-1	1.5-2.0 mg cm^{-2}	6
PCN-6 (1267.29 m^2 g^{-1})	120 mAh g^{-1} at 0.1 A g^{-1}	76 mAh g^{-1} at 10 A g^{-1}	1-2 mg cm^{-2}	7
NPC (1197.91 m^2 g^{-1})	158.2 mAh g^{-1} at 0.25 A g^{-1}	85 mAh g^{-1} at 10 A g^{-1}	~2.0 mg cm^{-2}	8
PSR-4 (2072 m^2 g^{-1})	88 mAh g^{-1} at 0.1 A g^{-1}	58.1 mAh g-1 at 5 A g^{-1}	~1.4 mg cm^{-2}	9

Table S3 The ion diffusion resistance (σ) and ion diffusion coefficient (D) of PCNs-

700, PCNs-800, and PCNs-900 (Average of three test).

Samples	ion diffusion resistance (σ)/ Ω $s^{-0.5}$	ion diffusion coefficient (D)/ cm^2 s^{-1}
PCNs-700	31.3±0.1	(7.2±0.1)× 10^{-10}
PCNs-800	28.7±0.1	(8.5±0.1)× 10^{-10}
PCNs-900	40.8±0.1	(4.2±0.1)× 10^{-10}

Reference

1. W. Jian, W. Zhang, X. Wei, B. Wu, W. Liang, Y. Wu, J. Yin, K. Lu, Y. Chen, H. N.

Alshareef and X. Qiu, *Advanced Functional Materials*, 2022, **32**, 2209914.
2. H. Ma, H. Chen, M. Wu, F. Chi, F. Liu, J. Bai, H. Cheng, C. Li and L. Qu, *Angewandte Chemie International Edition*, 2020, **59**, 14541-14549.
3. C. Zhu, R. Long, L. Zhu, W. Zou, Y. Zhang, Z. Gao, J. Shi, W. Tian, J. Wu and H. Wang, *Journal of Colloid and Interface Science*, 2023, **652**, 590-598.
4. Y. Zeng, F. Wei, Q. Liu, Y. Gao, S. Gao and Y. Lv, *Journal of Alloys and Compounds*, 2023, **963**, 171233.
5. K. Ning, M. Wei, Z. Jiang, T. Jiang, G. Zhao, L. Han, G. Zhu and Y. Zhu, *Materials Letters*, 2024, **355**, 135316.
6. D. Jia, Z. Shen, W. Zhou, Y. Li, J. He, L. Jiang, Y. Wei and X. He, *Chemical Engineering Journal*, 2024, **485**, 149820.
7. X. Zhang, J. Zhang, H. Zhang, L. Sun and Y. Zhang, *Journal of Energy Storage*, 2024, **92**, 112002.
8. C. Liu, X. Chang, H. Mi, F. Guo, C. Ji and J. Qiu, *Carbon*, 2024, **216**, 118523.
9. Z. Sun, X. Jiao, S. Chu and Z. Li, *ChemistrySelect*, 2023, **8**, e202304071.